PNAS RESEARCH ARTICLE | NEUROSCIENCE OPEN ACCESS

Female sexual behavior is disrupted in a preclinical mouse model of PCOS via an attenuated hypothalamic nitric oxide pathway

Mauro S. B. Silva[a], Laurine Decoster[a,1], Sara Trova[a,1], Nour E.H. Mimouni[a], Virginia Delli[a], Konstantina Chachlaki[a], Qiang Yu[b], Ulrich Boehm[b], Vincent Prevot[a], and Paolo Giacobini[a,2]

Edited by Donald Pfaff, Rockefeller University, New York, NY; received March 2, 2022; accepted June 14, 2022

Women with polycystic ovary syndrome (PCOS) frequently experience decreased sexual arousal, desire, and sexual satisfaction. While the hypothalamus is known to regulate sexual behavior, the specific neuronal pathways affected in patients with PCOS are not known. To dissect the underlying neural circuitry, we capitalized on a robust preclinical animal model that reliably recapitulates all cardinal PCOS features. We discovered that female mice prenatally treated with anti-Müllerian hormone (PAMH) display impaired sexual behavior and sexual partner preference over the reproductive age. Blunted female sexual behavior was associated with increased sexual rejection and independent of sex steroid hormone status. Structurally, sexual dysfunction was associated with a substantial loss of neuronal nitric oxide synthase (nNOS)-expressing neurons in the ventromedial nucleus of the hypothalamus (VMH) and other areas of hypothalamic nuclei involved in social behaviors. Using in vivo chemogenetic manipulation, we show that nNOS^{VMH} neurons are required for the display of normal sexual behavior in female mice and that pharmacological replenishment of nitric oxide restores normal sexual performance in PAMH mice. Our data provide a framework to investigate facets of hypothalamic nNOS neuron biology with implications for sexual disturbances in PCOS.

PCOS | AMH | sexual behavior | nitric oxide | hypothalamus

Significance

Polycystic ovary syndrome (PCOS) is a major endocrine disorder leading to female infertility worldwide. Patients with PCOS also often experience sexual dysfunction; however, the developmental and central mechanisms mediating this behavioral derangement are unclear. Here, we show that prenatal excess of anti-Müllerian hormone triggers PCOS-like impairment in female sexual behavior in mice. Sexual dysfunction in PCOS-like mice is associated with decreased expression of progesterone-sensitive neuronal nitric oxide synthase (nNOS) neurons in the hypothalamus. Chemogenetic inhibition of nNOS neuronal activity in the ventromedial nucleus of the hypothalamus recapitulates PCOS-like sexual dysfunction. Of clinical relevance, administration of nitric oxide donor rescues normal sexual behavior in PCOS-like mice.

Polycystic ovary syndrome (PCOS) is a highly prevalent disease affecting 5 to 18% of women of reproductive age worldwide (1, 2). PCOS is diagnosed upon the presence of at least two out of three prime features: high circulating levels of androgens (hyperandrogenism), menstrual irregularities (oligo-anovulation), and polycystic-like ovarian morphology (2, 3). Beyond its implications leading to female infertility, the disease is associated with several metabolic disruptions, cardiovascular diseases, and psychosocial disorders (4). Among these neurological implications, it has become clear that approximately 30% or more of patients with PCOS experience sexual dysfunctions, with clinical studies reporting a high risk of low sexual arousal, desire, and satisfaction and impaired lubrication and orgasm (5–9). These symptoms allude to disturbances in brain circuits controlling sexual function in the context of PCOS.

Neural circuits driving female sexual behaviors are conserved among vertebrate species operating under the influence of sex steroid hormone modulation, which is paramount for partner interaction, receptivity, and sexual performance (10, 11). Indeed, gonadal sex hormones are implicated in shaping circuit architecture in the hypothalamus during development and activating these neonatally programmed circuits over reproductive adult life in many species (12–16). The hypothalamus integrates sensorial stimuli and autonomic arousal from endogenous sex drive cues (e.g., estrous phase, energy status, hormone milieu, genital stimulation) to convey this information to other brain areas and peripheral nerves (10, 17). The ventromedial nucleus of the hypothalamus (VMH) is considered the hub of specialized neurons, with intrinsic properties driving different components of sexual behavior (18–21). The VMH harbors neurons expressing neuronal nitric oxide synthase (nNOS), the enzyme responsible for the production of nitric oxide (NO), a key gaseous neurotransmitter that stimulates female sexual behavior (22, 23) and communicates with other circuits within the social brain (24, 25). Despite current advances unraveling novel pathways in the female sexual brain with specific behavioral responses, there is a clear lack of knowledge on how disturbances in these circuits may participate in sexual dysfunctions affecting one-third of women with PCOS.

Growing evidence indicates that androgen excess *in utero* induces a developmental reprogramming of the female fetal brain toward the manifestation of PCOS traits later in life (26–29). Some studies have suggested that the clinical signs of hyperandrogenism

Competing interest statement: P.G., M.S.B.S, K.C., and V.P. disclose that they are inventors of a submitted patent application by the Institut National de la Santé et de la Recherche Médicale (INSERM) covering methods for treatment of sexual dysfunctions in PCOS.

This article is a PNAS Direct Submission.

Copyright © 2022 the Author(s). Published by PNAS. This open access article is distributed under Creative Commons Attribution-NonCommercial-NoDerivatives License 4.0 (CC BY-NC-ND).

[1]L.D. and S.T. contributed equally to this work.

[2]To whom correspondence may be addressed. Email: paolo.giacobini@inserm.fr.

This article contains supporting information online at http://www.pnas.org/lookup/suppl/doi:10.1073/pnas.2203503119/-/DCSupplemental.

Published July 22, 2022.

Downloaded from https://www.pnas.org by UNIVERSITEIT VAN AMSTERDAM UVA on April 14, 2025 from IP address 145.18.161.224.

have detrimental sexual effects (5), indicating a negative correlation between androgen levels and sexual function in PCOS. In recent years, it has been proposed that prenatal anti-Müllerian hormone excess may trigger gestational hyperandrogenism via the inhibition of placental aromatase (29, 30) and that women with PCOS display higher circulating levels of androgens and AMH during pregnancy as compared to healthy women (29, 31). Prenatal AMH-treated mice (PAMH) reliably recapitulate all the mouse equivalents of the PCOS Rotterdam criteria (29, 32) and are thus a preclinical model to mimic the human PCOS condition. PAMH female mice also display pronounced neuroendocrine dysfunction leading to exacerbated luteinizing hormone (LH) secretion (29), as in women with PCOS (33), denoting the presence of prenatally reprogrammed defects within the gonadotropin-releasing hormone (GnRH) neuronal network. Thus, prenatal AMH excess–mediated disruptions in the female brain may be key to understanding the pathophysiology of PCOS.

Here, we investigated whether prenatal AMH excess could underpin defects in sex circuits promoting sexual dysfunction in PCOS-like female mice. We uncovered a profound decrease of nNOS and progesterone receptor (PR) expression in the VMH. These anatomical changes were also associated with significant impairment of sexual receptivity in PCOS-like female mice. Nevertheless, normal sexual function in PAMH female mice was restored to control levels upon peripheral injection of NO donor. Performing a series of acute functional manipulations in freely moving female mice, we showed that chemogenetic silencing of $nNOS^{VMH}$ neurons in control female mice recapitulates PCOS-like sexual dysfunctions. Taken together, we unveiled a brain pathway potentially underpinning the etiology of low sexual drive in PCOS while pointing to prospective therapeutic approaches to rescue normal sexual function in these women.

Results

PCOS-like Animals Show Altered Sexual Behavior. To date, alterations in female sexual behavior in preclinical models of PCOS are not well described. Here, we generated PAMH female mice (29) and performed a thorough neuroanatomical and behavioral assessment of these animals (Fig. 1*A*). We confirmed that adult PAMH female mice present with a substantial disruption of reproductive cycles, wherein PAMH animals spend less time in proestrus, the preovulatory stage ($P < 0.0001$), and more time in metestrus ($P < 0.05$) than control female mice (*SI Appendix*, Fig. S1 *B* and *C*). Hyperandrogenemia is a hallmark of PCOS (34) and preclinical PCOS models (32); however, circulating testosterone levels are commonly measured over the light phase of light:dark cycles. We assessed plasma testosterone levels on the day of estrus (receptive phase) over the dark phase, when naturally nocturnal mice display full sexual behavior. We found that PAMH female mice have higher plasma testosterone levels (~8.62-fold increase) than control female mice (*SI Appendix*, Fig. S1*E*). Neuroendocrine disruptions contribute to increased testosterone production through high LH pulse secretion and, hence, LH actions in PCOS ovaries (28, 33). We found that diestrous PAMH mice exhibit high pulsatile LH secretion over the dark phase of the light:dark cycles (*SI Appendix*, Fig. S1*F*). Specifically, PAMH female mice exhibit higher mean LH levels (*SI Appendix*, Fig. S1*G*), pulse frequency of LH release (*SI Appendix*, Fig. S1*H*), and integrated LH response (*SI Appendix*, Fig. S1*I*) than control female mice.

Copulatory behavior in female rodents is typically displayed as lordosis over the consummatory phase, being primarily dependent upon the proper functioning of brain circuitry. Thus, female mice were tested for lordosis behavior to determine whether the PAMH insult also promotes the disruption of sexual receptivity and performance in adulthood (Fig. 1). PAMH female mice displayed significantly fewer lordosis responses compared with control female mice (Fig. 1*B*). This disruption in sexual behavior was not attributed to a loss of mating partner's interest as male mice attempted to mount PAMH female mice more often than control female mice (Fig. 1*C*). The latency for the first mount was not different between the groups, taking on average 309.4 ± 148.2 s for the first mounting attempt in males paired with control female mice vs. 408.8 ± 110.2 s for males paired with PAMH female mice (Mann–Whitney *U* test; $P = 0.58$).

Decreased sexual motivation and performance are frequently associated with high levels of anxiety in both healthy women and women with PCOS (35). Thus, we tested whether PAMH treatment could also promote anxiety-like behavior as a primary culprit of sexual dysfunction by employing the elevated plus maze (EPM) test, in which spending less time in open areas of the maze is a valid index of anxiety-like behavior (36). Analysis indicated that PAMH treatment does not affect the time spent in open areas, such as the open arm and the central part of the maze (*SI Appendix*, Fig. S2*A*). We observed a mild increase in the time spent in the closed arms of the maze by PAMH female mice compared with control mice (*SI Appendix*, Fig. S2*B*). Increased time in closed arms could indicate a normal proclivity toward dark enclosed areas following risk assessment and avoidance of open spaces. However, we also did not detect any differences in the number of entries in either the closed or the open arms (*SI Appendix*, Fig. S2 *B* and *C*). The ratio of time spent in the open arms compared to the other areas of the maze (*SI Appendix*, Fig. S2*D*) and the latency to enter the open arms (*SI Appendix*, Fig. S2*E*) were also similar between the two groups. Together, our findings reveal that PAMH female mice display a pronounced impairment of sexual performance, which is unlikely to be related to an anxiety-like condition.

Sexual Dysfunction and Sexual Rejection Behaviors Are Not Dependent upon Circulating Ovarian Hormone Levels in PCOS-like Mice. Ovarian steroid hormone actions in the female brain by estradiol (E2) and progesterone (P4) are necessary to increase sexual motivation and the display of adequate lordosis behavior (37), respectively. Thus, differences in endogenous E2 and P4 levels could influence lordosis behavior in PAMH female mice. To investigate this possibility, we assessed lordosis behavior in control and PAMH female mice before (intact) and after ovariectomy followed by E2 and P4 supplementation. We found that E2+P4 treatment does not affect lordosis behavior in both groups and that PAMH female mice still display impaired sexual behavior in comparison with control female mice (Fig. 1*D*; effect of the E2+P4 treatment: $P = 0.73$, $F_{1,24} = 0.12$; effect of the phenotype: $P < 0.0001$, $F_{1,24} = 148.00$). These results suggest that intrinsic defects may arise from developmental disruptions in the PCOS-like condition, most likely impinging on the E2/P4 signaling pathways, and that sex hormone replenishment in adulthood is not sufficient to recover normal sexual performance.

Social interactions between female and male mice toward copulation are facilitated when female mice are highly receptive. Conversely, during unreceptive states, female mice may display rejecting behaviors in response to male mounting attempts. Based on previous reports (38, 39), we categorized these sexual rejection

Downloaded from https://www.pnas.org by UNIVERSITEIT VAN AMSTERDAM UVA on April 14, 2025 from IP address 145.18.161.224.

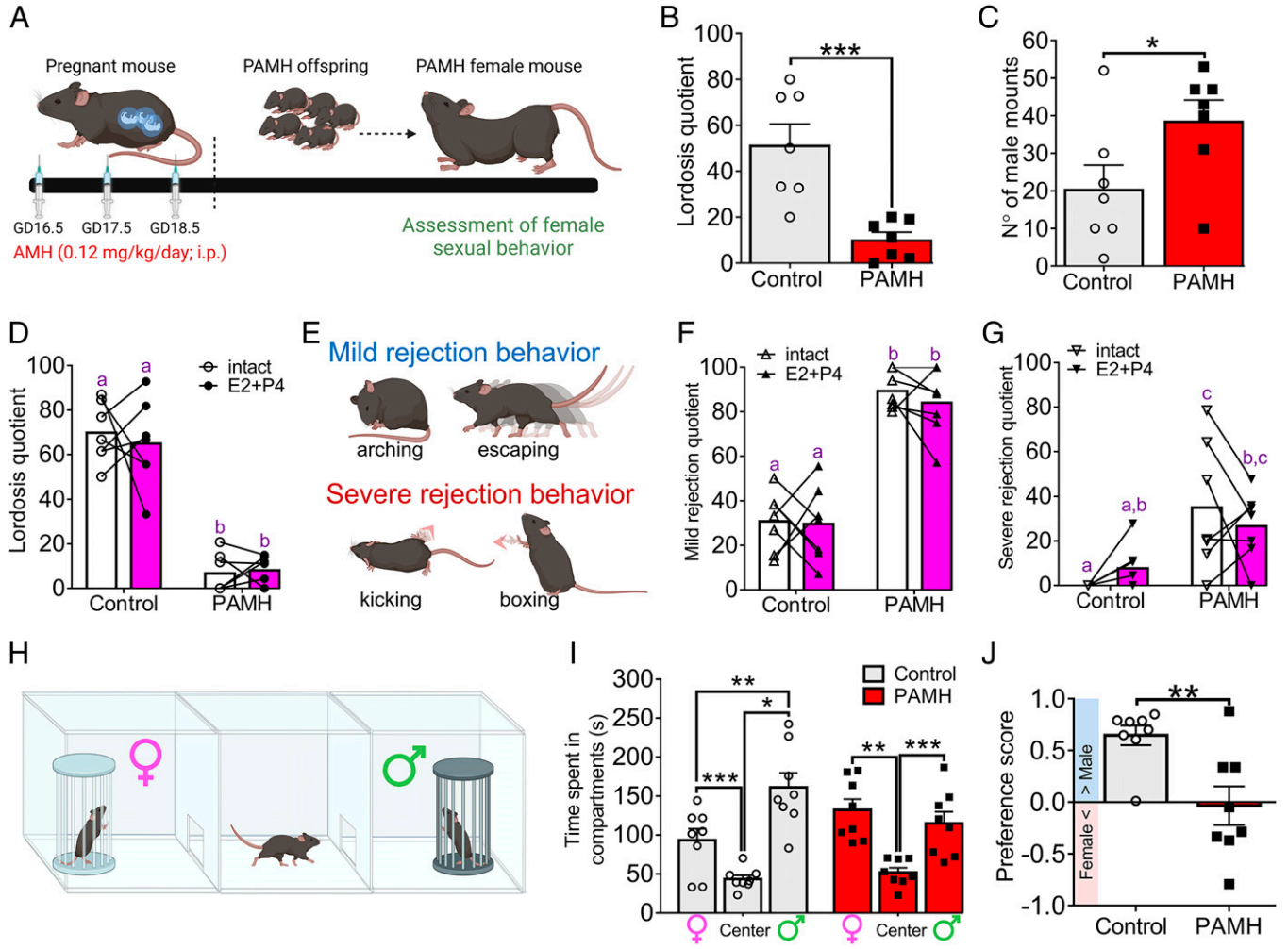

Fig. 1. PAMH female mice display sexual dysfunction during adulthood. (*A*) Schematic representation of PAMH modeling. (*B*) LQ in control ($n = 7$) and PAMH ($n = 7$) female mice. Unpaired Student's *t* test; $^{***}P < 0.001$. GD: gestational age. (*C*) Number of male mounting trials over the 15-min lordosis test. Males were paired with control ($n = 7$) and PAMH ($n = 7$) female mice. Unpaired Student's *t* test; $^{*}P < 0.05$. (*D*) LQ from paired intact and ovariectomized female mice with estradiol (E2)/progesterone (P4) supplementation (E2+P4) in control ($n = 7$) and PAMH ($n = 7$) groups. Two-way ANOVA with Tukey's posthoc test. (*E*) Representation of sexual rejection behaviors in female mice such as mild rejection (arching and escaping) and severe rejection (kicking and boxing) behavior. (*F* and *G*) MRQ and SRQ in paired intact and ovariectomized female mice treated with E2+P4 in control ($n = 7$) and PAMH ($n = 7$) groups. Two-way ANOVA with Tukey's posthoc test. (*H*) Drawing shows how mate preference test was performed in female mice. (*I*) The time spent by control ($n = 8$) and PAMH ($n = 8$) female mice exploring the different compartments of the mate preference test box. Two-way ANOVA with Tukey's posthoc test; $^{*}P < 0.05$, $^{**}P < 0.01$; $^{***}P < 0.001$. (*J*) Preference score for mate preference test in control ($n = 8$) and PAMH ($n = 8$) female mice. The blue bar indicates male-directed preference while the pink bar indicates female-directed preference. Unpaired Student's *t* test; $^{**}P < 0.01$. Data are represented as mean ± SEM. Different letters indicate statistically different groups.

behaviors into two types: mild rejection, in which female mice display either arching of the back to prevent mounting or escaping, and severe rejection, when female mice engage with hindlimb kicking and boxing following mounting attempts (Fig. 1*E*). We observed that while intact control female mice in estrus display a low mild rejection quotient (MRQ = 30.2) and severe rejection quotient (SRQ = 3.8), intact PAMH female mice in estrus spend more time rejecting male mounts with high rates of both mild (MRQ = 86.7) and severe (SRQ = 30.8) rejecting behaviors (Fig. 1*F* and *G*). We also observed that hormone supplementation does not change the magnitude of these behaviors in both groups for either mild (effect of the E2+P4 treatment: $P = 0.53$, $F_{1,24} = 0.39$) or severe rejection (effect of the E2+P4 treatment: $P = 0.96$, $F_{1,24} = 0.003$) in comparison with when the same animals were first tested in intact estrus (Fig. 1*F* and *G*).

Because PAMH mice present a robust disruption of sexual performance and enhanced display of rejecting behaviors, we also investigated whether the mate preference was altered in these animals. We assessed mate preference using a two-chamber test in which one side contained a sexually-experienced and receptive female mouse and the opposite side contained asexually-experienced male mouse (Fig. 1*H*). Group analysis revealed that control female mice spend more time exploring the chamber with an experienced male, whereas PAMH female mice spend a similar amount of time exploring both chambers (Fig. 1*J*). Further analysis confirmed that unlike control female mice, which present a typical male-directed preference, PAMH females fail to show any sex-directed preference (Fig. 1*I*). This loss of male-directed preference may contribute to the impairment in sexual function observed in PAMH female mice.

Sexual Dysfunction in PAMH Mice Is Associated with Decreased Expression of nNOS and PR in the Hypothalamus. Among multiple signal transduction pathways governing female sexual behavior, both NOergic signaling and progesterone actions are well known to trigger female lordosis (22, 37, 40, 41). Women with PCOS have both low circulating levels of NO metabolites (42, 43) and impaired progesterone-mediated negative feedback (33, 44). Therefore, we hypothesized that the expression of nNOS and PR could be disrupted in PAMH female mice as they

Downloaded from https://www.pnas.org by UNIVERSITEIT VAN AMSTERDAM UVA on April 14, 2025 from IP address 145.18.161.224.

exhibit both neuroendocrine and sexual dysfunction. We mapped the expression of nNOS and PR in different hypothalamic regions known to be involved in female sexual behavior (17, 21, 24, 45): the rostral periventricular area of the third ventricle (RP3V), the VMH, and the arcuate nucleus (ARN) during estrus.

First, we documented by immunohistochemical studies a robust ~50% reduction in the number of nNOS neurons located in the RP3V ($nNOS^{RP3V}$; Fig. 2*A*–*D*) in PAMH female mice compared with control female mice (Fig. 2*E*). The expression of PR in the RP3V (PR^{RP3V}) was not altered by PAMH treatment (Fig. 2*F*), whereas the number of $nNOS^{RP3V}$ neurons coexpressing PR was significantly lower in PAMH mice than in controls (Fig. 2*G*; 61.7% lower in PAMH; $P < 0.0001$). The percentage of colocalization between $nNOS^{RP3V}$ and PR^{RP3V} was similar in both groups (Fig. 2*H*; $P = 0.66$; control = 47.22 ± 1.5% vs. PAMH = 40.91 ± 7.2%).

Next, we investigated the expression of both proteins in the VMH, which is highly important for progesterone-mediated sexual performance in female mice (19, 21) and the integration of neuroendocrine functions (Fig. 2*I*–*L*). We discovered that PAMH female mice exhibit 44.5% fewer nNOS neurons in the VMH ($nNOS^{VMH}$) when compared with controls (Fig. 2*M*). A similar shift was also observed for both cells expressing PR (PR^{VMH}) (Fig. 2*N*; 52.2% reduction; $P < 0.0001$) and $nNOS^{VMH}$ neurons coexpressing PR (Fig. 2*O*; 43.4% reduction; $P < 0.01$) in PAMH female mice compared with control female mice. Although these protein expressions were attenuated in PAMH mice, the percentage of $nNOS^{VMH}$ expressing PR^{VMH} colocalization was similar between the groups (Fig. 2*P*; control = 61.3% vs. PAMH = 64.3%; $P = 0.69$), indicating that the reduction of the number of PR^{VMH} cells may be dependent upon the reduction of $nNOS^{VMH}$ expression.

We then investigated whether the expression of nNOS and PR in the ARN ($nNOS^{ARN}$ and PR^{ARN}, respectively) (Fig. 2*Q*–*T*) could be disturbed in a PCOS-like condition. Immunohistochemical analysis showed that the number of $nNOS^{ARN}$ neurons (Fig. 2*U*), PR^{ARN} cells (Fig. 2*V*), and $nNOS^{ARN}$ neurons coexpressing PR (Fig. 2*W*) were significantly lower in PAMH mice than control mice. The ARN is an elongated region stretching caudally throughout the medial basal hypothalamus; thus, we carried out a refined analysis of different parts of the ARN to identify specific regions with abnormal nNOS and PR expression. The lower number of $nNOS^{ARN}$ neurons in PAMH female mice was due to a robust decrease in the middle part of the nucleus (mARN; bregma = −1.55 mm ↔ −2.03 mm; $P < 0.01$), whereas the rostral (rARN; bregma = −1.23 mm ↔ −2.03 mm) and caudal parts (rARN; bregma = −2.03 mm ↔ −2.53 mm) did not seem to be significantly affected by PAMH treatment (*SI Appendix*, Fig. S3*A*). Meanwhile, PR expression was decreased along with the entire extension of the ARN in PAMH female mice (*SI Appendix*, Fig. S3*B*). The percentage of coexpression of PR and nNOS was the lowest among the three hypothalamic regions for both groups (Fig. 2*X*), and the number of $nNOS^{ARN}$ neurons coexpressing PR was only significantly decreased in the mARN region (*SI Appendix*, Fig. S3*C*).

We further analyzed the percentage of PR cells coexpressing nNOS in the three hypothalamic nuclei. We found that within each nucleus, control and PAMH female mice express similar percentages of coexpression of the two proteins in PR cells (*SI Appendix*, Fig. S3*D*). Among the three nuclei, the VMH contained the highest colocalization rate with 91.6 ± 2.5% and 92.1 ± 3.6% of PR cells coexpressing nNOS in control and PAMH mice, respectively (*SI Appendix*, Fig. S3*D*; effect of hypothalamic nuclei: $F_{2,30} = 216.7$; $P < 0.0001$). PR^{RP3V} cells coexpressed 43.3 ± 6.9% and 32.12 ± 6.9% in control and PAMH mice, respectively, whereas the ARN displayed the lowest colocalization rate with 5.6 ± 0.9% and 5.0 ± 1.2% in control and PAMH mice, respectively (*SI Appendix*, Fig. S3*D*). Because gonadal hormones influence the expression of nNOS in hypothalamic and limbic regions in both sexes in different mammalian species (46), we further examined whether the hyperandrogenism of PAMH animals could negatively impact nNOS expression in other brain regions involved in the control of sexual behavior. Histological analysis from brain sections containing the medial preoptic area (MPA), median preoptic nucleus (MnPO), anterior division of the bed nucleus of the stria terminalis (aBNST), and posterodorsal medial amygdala nucleus (pdMeA) did not reveal any difference in the number of nNOS neurons in these regions between control and PAMH female mice (*SI Appendix*, Table S1). Taken together, these data illustrate a robust association between neuroendocrine and sexual behavior impairments with a disruption of nNOS and PR expression in the hypothalamus of PCOS-like female mice.

Peripheral Injection of NO Donor Restores Normal Sexual Behavior and Attenuates Sexual Rejection in PAMH Mice. Previous reports indicate that the control of female sexual behavior is highly dependent upon NOergic signaling in rodents (22–24). Having established the loss of nNOS expression in hypothalamic sites in PAMH mice, we next addressed whether the replenishment of NO levels could rescue normal sexual function. Control and PAMH female mice were injected with either saline or S-nitroso-*N*-acetylpenicillamine (SNAP; 8mg/kg), a well-known NO donor to boost circulating NO levels. Saline-injected PAMH mice displayed the previously observed impairment in lordosis behavior in comparison with saline-injected controls (Fig. 3*A*). The administration of SNAP prior to testing robustly recovered normal lordosis behavior in PAMH female mice similar to control levels (Fig. 3*A*; effect of SNAP treatment: $P < 0.0001$, $F_{1,34} = 52.29$). The recovery of lordosis behavior reached an approximated 7.28-fold increase in PAMH female mice following SNAP treatment (lordosis quotient; $LQ_{PAMH+saline} = 9.37 \pm 2.48$ vs. $LQ_{PAMH+SNAP} = 68.17 \pm 6.97$). Concurrently, SNAP administration significantly reduced both mild (Fig. 3*B*) and severe (Fig. 3*C*) rejection behaviors in PAMH female mice similar to control levels, while it did not change these parameters in control female mice (effect of SNAP treatment for MRQ: $P < 0.0001$, $F_{1,34} = 27.71$; effect of SNAP treatment for SRQ: $P < 0.0001$, $F_{1,34} = 40.47$).

We aimed to determine how 8 mg/kg SNAP treatment may change the neuronal activation landscape in the female brain in estrus control and PAMH mice following the lordosis test. We chose to evaluate the percentage of cells expressing cFOS, an immediate early gene product and proxy of enhanced neuronal activity, in hypothalamic and limbic areas that share either direct or indirect connectivity with the VMH (24, 47, 48) and are involved in the control of both appetitive and consummatory aspects of sexual behavior (49–52): the RP3V, MPA, MnPO, aBNST, ARN, pdMeA, dorsomedial hypothalamus (DMH), ventrolateral and dorsomedial periaqueductal gray matter (vlPAG, dmPAG), and ventral tegmental area (VTA; *SI Appendix*, Fig. S4*A*). The percentage of cells expressing cFOS was also examined within the ventrolateral VMH (vlVMH) and dorsomedial VMH subregions (dVMH; *SI Appendix*, Fig. S4*B*). We found that vehicle-treated estrous PAMH female mice had a significantly lower percentage of cFOS expression within the MPA, MnPO, vlVMH, and pdMeA compared with control animals treated with either vehicle or SNAP (*SI Appendix*, Fig. S4*C*).

Downloaded from https://www.pnas.org by UNIVERSITEIT VAN AMSTERDAM UVA on April 14, 2025 from IP address 145.18.161.224.

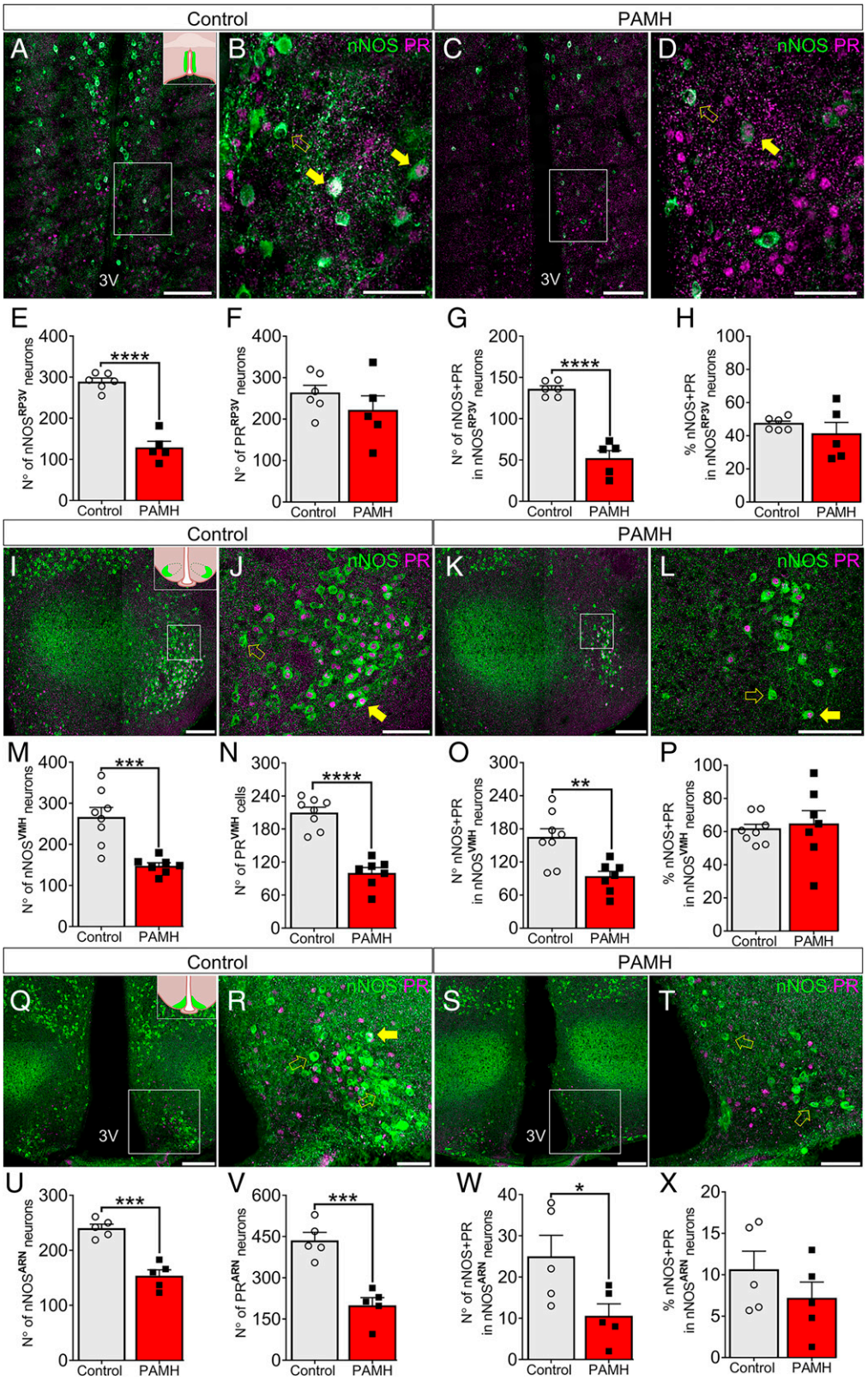

Fig. 2. Sexual dysfunction in PAMH mice is associated with decreased expression of neuronal nNOS and PR in the hypothalamus. (*A*–*D*) Representative images of the RP3V. (*E*–*G*) Number of nNOS-, PR-, and nNOS+PR-expressing cells in the RP3V in control ($n = 6$) and PAMH ($n = 5$) female mice. Unpaired Student's *t* test. (*H*) Percentage of nNOS neurons coexpressing PR in the RP3V in control ($n = 6$) and PAMH ($n = 5$) female mice. Mann–Whitney *I* test. (*I*–*L*) Representative images of the VMH. (*M*–*O*) Number of nNOS-, PR-, and nNOS+PR-expressing cells in the VMH in control ($n = 8$) and PAMH ($n = 7$) female mice. Unpaired Student's *t* test. (*P*) Percentage of nNOS neurons coexpressing PR in the VMH in control ($n = 8$) and PAMH ($n = 7$) female mice. Mann–Whitney *U* test. (*Q*–*T*) Representative images of the ARN. (*U*–*W*) Number of nNOS-, PR-, and nNOS+PR-expressing cells in the ARN in control ($n = 5$) and PAMH ($n = 5$) female mice. Unpaired Student's *t* test. (*X*) Percentage of nNOS neurons coexpressing PR in the ARN in control ($n = 5$) and PAMH ($n = 5$) female mice. Mann–Whitney *U* test. The white dashed boxes indicate the region of a high-magnification image. Full yellow arrows show examples of colocalization between nNOS and PR immunoreactivity, whereas hollow yellow arrows point to nNOS expression only. Data are represented as mean ± SEM; $*P < 0.05$; $**P < 0.01$; $***P < 0.001$; $****P < 0.0001$ (Inset boxes in *A*, *I*, and *Q* show in light green the position of the RP3V, VMH, and ARN, respectively, within the mouse brain from a coronal view. White scale bars in *A*, *C*, *I*, *K*, *Q*, and *S*, 100 μm; white scale bars in *B*, *D*, *J*, *L*, *R*, and *T*, 50 μm).

Downloaded from https://www.pnas.org by UNIVERSITEIT VAN AMSTERDAM UVA on April 14, 2025 from IP address 145.18.161.224.

Remarkably, SNAP administration increased cFOS expression in all four regions in PAMH mice to control levels (*SI Appendix*, Fig. S4*C*). In both regions of the PAG, SNAP-treated control mice displayed lower cFOS expression compared with vehicle-treated control mice, whereas SNAP treatment did not alter cFOS expression in these regions in either PAMH mice group (*SI Appendix*, Fig. S4*C*). Evaluation of the proportion of nNOS neurons expressing cFOS in each of these areas revealed that only a small portion of nNOS neurons expressed cFOS in vehicle-treated PAMH mice in the vlVMH (7.92 ± 4.88%) and pdMeA (3.78 ± 3.40%) following the lordosis test. SNAP treatment of PAMH mice fully restored the proportion of nNOS cells expressing cFOS to control levels (*SI Appendix*, Fig. S4*D*). These results indicate that SNAP-mediated amelioration of sexual dysfunction in PAMH female mice may result from the recovery of normal neuronal activation in the hypothalamic and limbic structures in the female brain involved in sexual behavior.

NO-mediated physiological responses are mostly dictated by intracellular levels of cyclic guanosine monophosphate (cGMP). Sildenafil citrate, commercialized as Viagra, is a commonly used drug for male sexual dysfunction, and it works enhancing NOergic signaling by decreasing the degradation of cGMP and thus leading to the accumulation of intracellular levels of cGMP . To determine the severity of NO insufficiency in PAMH mice, we administered sildenafil citrate to both groups and evaluated lordosis behavior. Sildenafil citrate treatment did not rescue normal lordosis behavior in PAMH mice (Fig. 3*D*; effect of sildenafil citrate treatment: $P = 0.45$, $F_{1,28} = 0.57$). We also observed that sildenafil citrate treatment was not effective to attenuate either mild (Fig. 3*E*) or severe (Fig. 3*F*) rejection behaviors in PAMH mice. Together, our results point to severe NO deficiency in PAMH mice and suggest a potential therapeutic approach to rescue normal sexual function in PCOS based on enhancing NO production rather than controlling the downstream cGMP levels.

Chemogenetic Silencing of nNOS^{VMH} Neurons Recapitulates PCOS-like Sexual Dysfunction. Among the three hypothalamic areas investigated in our study, the VMH (nNOS^{VMH}) is considered the NOergic output responsible for controlling sexual performance in mammalian females (22), whereas nNOS^{RP3V} and nNOS^{ARN} are likely to contribute to the neuroendocrine control of GnRH/LH secretion (53). PR^{VMH} neurons are also known to participate in female sexual behavior (19), and here we demonstrated that approximately 60% of the nNOS^{VMH} neuronal population coexpress PR. Hence, we focused our investigations on examining whether acute chemogenetic inhibition of nNOS^{VMH} neurons would promote the impairment of sexual function such as that observed in PAMH female mice. To this end, we selectively targeted the expression of the designer receptors exclusively activated by designer drugs (DREADD)–based tool hM4(Gi) into the VMH of *Nos1*$^{cre/+}$ (*Nos1-ires-cre*; B6.129-*Nos1*$^{tm1(cre)Mgmj}$/J) female mice (*SI Appendix*). Viral transfection was established using a Cre-recombinase-dependent adeno-associated virus serotype 9 in which hM4(Gi) is fused with the mCherry reporter under the control of the human synapsin (hSyn) promoter (AAV9-hSyn-DIO-hM4D(Gi)-mCherry) (Fig. 3*G*). The control group was composed of wild-type female mice receiving the same stereotaxic surgery. This approach provided an average efficiency of 86.82 ± 2.33% of nNOS^{VMH} neurons targeted with the inhibitory DREADD and with an off-target infection rate of 5.48 ± 2.17% in non-nNOS^{VMH} neurons (Fig. 3*H*–*O*).

Following viral transfection, *Nos1*$^{cre/+}$ female mice were subjected to two lordosis tests and randomly received either vehicle or the DREADD ligand clozapine *N*-oxide (CNO; 3 mg/kg) one hour before behavioral assessment. We discovered that acute inhibition of nNOS^{VMH} neurons with CNO markedly impaired lordosis behavior (Fig. 3*P*; $LQ_{vehicle} = 67.39 \pm 6.13$ vs. $LQ_{CNO} = 4.24 \pm 2.26$; $P < 0.01$; Wilcoxon signed-rank test) compared with vehicle injection. Over the same assessment frame, CNO-injected mice displayed higher mild (Fig. 3*Q*) and severe (Fig. 3*R*) rejection behaviors than vehicle-injected mice. The control group did not show any difference between treatments when analyzing either lordosis (*SI Appendix*, Fig. S5*A*), mild rejection (*SI Appendix*, Fig. S5*B*), or severe rejection behaviors (*SI Appendix*, Fig. S5*C*). Our data indicate that the selective inhibition of nNOS^{VMH} neurons recapitulates the observed sexual dysfunction and enhancement of rejection behaviors of our PCOS preclinical mouse model. These results also reveal that nNOS^{VMH} neurons are functionally required for the display of female sexual behavior in mice.

Kisspeptin Does Not Rescue Normal Sexual Behavior following Acute Inhibition of nNOS^{VMH} Neurons. Recent reports support the idea that kisspeptin, widely known for its role in the neuroendocrine control of fertility, stimulates female sexual behavior (23, 24). It is suggested that this kisspeptidergic drive may be upstream to nNOS^{VMH} neurons and located in the RP3V region (Kiss1^{RP3V}) (24). However, the RP3V is also a target of PR-expressing VMH (PR^{VMH}) neurons triggering female sexual behavior in an estrus-dependent manner (15). Here, we aimed to dissect the requirement of the coupling kisspeptin–nNOS^{VMH} neurons for the display of normal sexual behavior and whether the disruption of this pathway recapitulates PCOS-like sexual dysfunction.

Using a similar approach as described above, we stereotaxically delivered the expression of AAV9-hM4(Gi)-mCherry in nNOS^{VMH} neurons in both *Nos1*$^{cre/+}$ and wild-type female mice. Following viral transfection, all sexually experienced estrous female mice were exposed to three lordosis behavioral tests before commencing treatments. Each animal was subjected to different treatments applying a preinjection (-60 min) with either vehicle or CNO followed by injection (-30 min) with vehicle or kisspeptin-10 (0.52 μg/kg) before the lordosis test (Fig. 4*A*). In control female mice, CNO alone did not have any effect on the behavioral output, while kisspeptin injection significantly enhanced lordosis performance (Fig. 4*B*). In *Nos1*$^{cre/+}$ female mice, pretreatment CNO caused significant disruption of sexual behavior and kisspeptin injection was not able to reverse this condition (Fig. 4*B*).

Previously, our group showed that a certain degree of masculinization occurs within different hypothalamic nuclei in PAMH female mice (29). Here, we examined whether PAMH treatment affects progesterone-sensitive Kiss1^{RP3V} neurons. Using the reporter knock-in mouse line Kiss1-(IRES)-Cre$^{+/-}$/ROSA26-CAG-tauGFP$^{+/-}$ (Kiss1-GFP), in which the expression of Cre recombinase enzyme is dependent upon the kisspeptin promoter, we generated control and PAMH female mice (Fig. 4*C*). This approach allowed the proper visualization of Kiss1 cell bodies, which is commonly challenging using traditional immunohistochemical approaches. Neuroanatomical analysis revealed that PAMH female mice had a significantly lower number of Kiss1^{RP3V} neurons when compared with control female mice (Fig. 4*D*; 65.3% of reduction; $P < 0.0001$). We could also detect a disruption in the number of Kiss1^{RP3V} neurons expressing PR in PAMH female mice in comparison with control female mice (Fig. 4*D*), although both groups presented a similar percentage of PR-expressing Kiss1^{RP3V} neurons (Fig. 4*E*). Further investigation revealed that kisspeptin and

Downloaded from https://www.pnas.org by UNIVERSITEIT VAN AMSTERDAM UVA on April 14, 2025 from IP address 145.18.161.224.

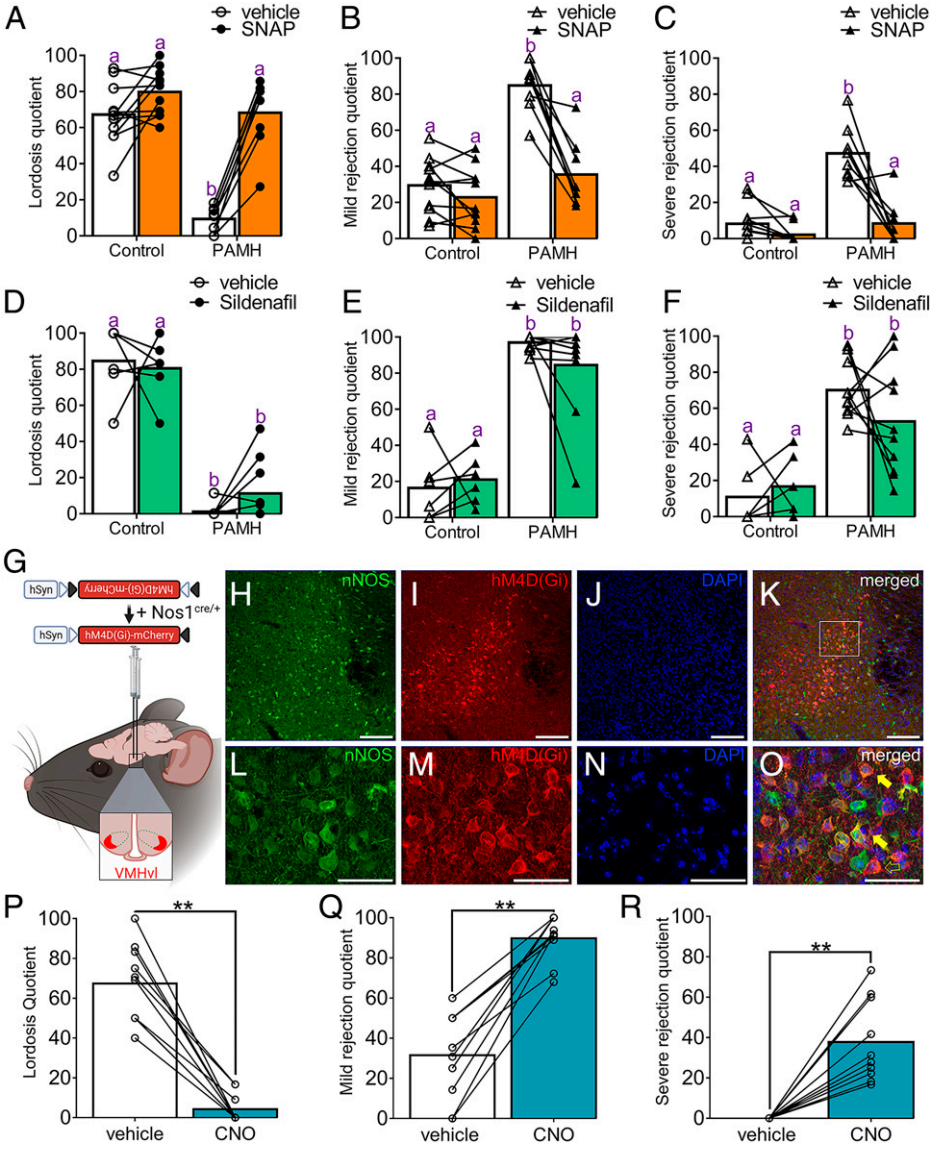

Fig. 3. Functional requirement of NOergic signaling and nNOS^{VMH} neurons for the control of female sexual behavior. (*A–C*) Lordosis, mild rejection, and severe rejection quotients following the administration of 8 mg/kg SNAP 15 min before the behavioral test in control (n = 11) and PAMH (n = 8) female mice. Two-way ANOVA with Tukey's posthoc test. (*D–F*) Lordosis, mild rejection, and severe rejection quotients following the administration of 15 mg/kg sildenafil citrate 1 h before the behavioral test in control (n = 6) and PAMH (n = 10) female mice. Two-way ANOVA with Tukey's posthoc test. (*G*) Schematic shows strategy for selective expression of AAV9-hM4D(Gi)-mCherry targeted to nNOS^{VMH} neurons in *Nos1*$^{cre/+}$ female mice. (*H–O*) Representative confocal images show viral transfection in the VMH of *Nos1*$^{cre/+}$ female mice. Images show nNOS (*H*), mCherry (*I*), nuclear marker DAPI (*J*), and colocalization immunoreactivity in the nucleus. (*L–O*) depict high-magnification images from (*H–K*), respectively, representing the area shown within the white dashed box in *K* . Full yellow arrows show examples of colocalization between nNOS and mCherry immunoreactivity, whereas hollow yellow arrows point to mCherry expression only. (*P–R*) Lordosis, mild rejection, and severe rejection quotients following chemogenetic inhibition of nNOS^{VMH} neurons in female mice. Acute chemogenetic manipulation with 3 mg/kg CNO promotes sexual dysfunction and enhanced sexual rejection in *Nos1*$^{cre/+}$ female mice (n = 10). Wilcoxon signed-rank test; $^{**}P < 0.01$. Data are represented as mean ± SEM. Different letters indicate statistically significant differences. Scale bars: *H-K*, 100 μm; *L-O*, 30 μm.

nNOS were mostly expressed in two distinct populations within the RP3V region (*SI Appendix*, Fig. S6 *A–F*), whereas only a small portion of neurons expressed both proteins similarly in control and PAMH female mice (*SI Appendix*, Fig. S6 *G* and *H*; control = 0.62% vs. PAMH = 0.83%). These data suggest that kisspeptin signaling is upstream of nNOS^{VMH} neuron–mediated lordosis behavior and that conjoint disrupted expression of both Kiss1^{RP3V} and nNOS^{VMH} may contribute to sexual dysfunction in PCOS.

Discussion

Clinical studies have identified the presence of impaired sexual function in nearly one-third of young women with PCOS (6, 8) showing significant sexual dysfunction, estimated as decreased sexual satisfaction, arousal, lubrication, and orgasm (8). This evidence suggests the existence of central impairments in the brains of women with PCOS.

The employment of preclinical models offers the unique opportunity to investigate the etiology of sexual dysfunction in PCOS, and PAMH mice have recently been used to understand neuroendocrine impairments (29, 54), infertility (29), and transgenerational epigenetic inheritance of the disease (30). Here, we confirm that this model is a robust translational tool to investigate reproductive dysfunction in PCOS. We report that androgen excess and high LH secretion, a proxy of high GnRH secretion, are also present over the dark phase of the light:dark cycles, when mice are most receptive to sexual intercourse and when we performed the

Downloaded from https://www.pnas.org by UNIVERSITEIT VAN AMSTERDAM UVA on April 14, 2025 from IP address 145.18.161.224.

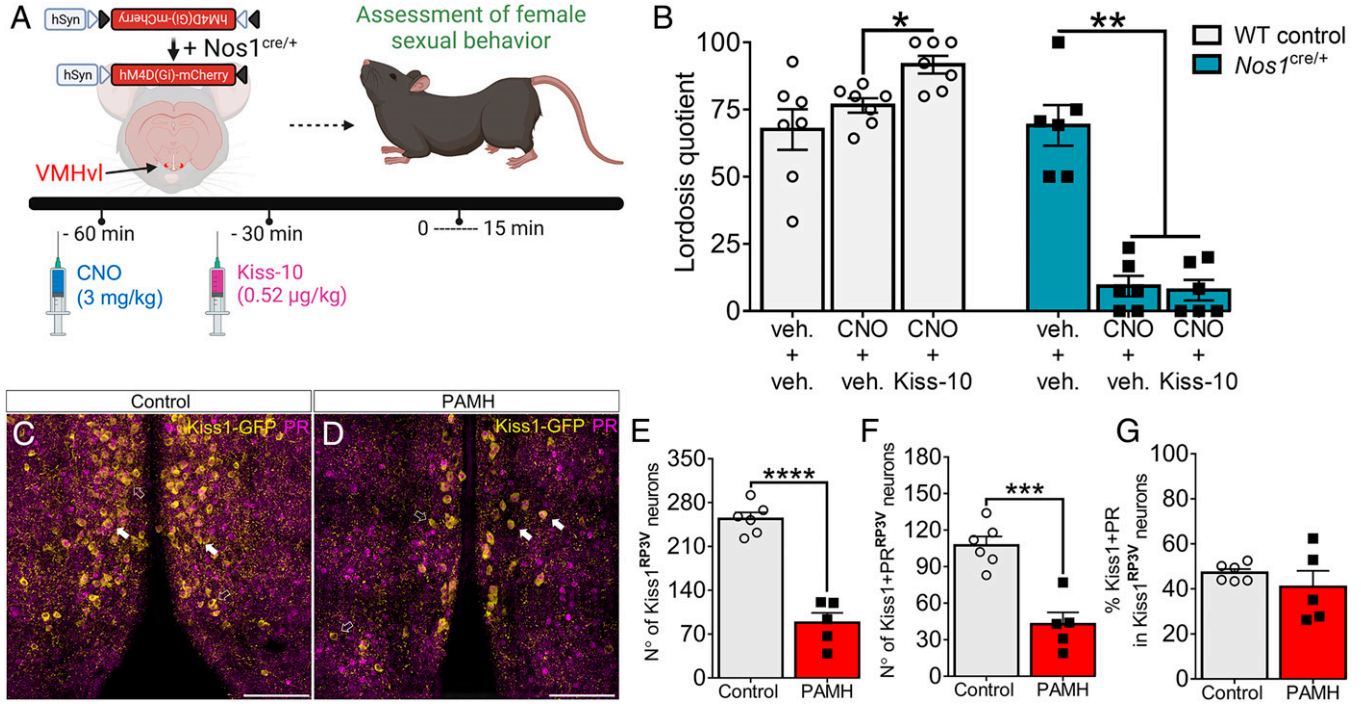

Fig. 4. Kisspeptin does not restore normal sexual behavior following acute inhibition of nNOS^{VMH} neurons. (*A*) Schematic shows *Nos1*$^{cre/+}$ female mice bilaterally injected with AAV9-hM4D(Gi)-mCherry targeting nNOS^{VMH} neurons. Wild-type (WT) control and *Nos1*$^{cre/+}$ female mice were subjected to a pretreatment with 3 mg/kg CNO (i.p.) and treatment with kisspeptin-10 (Kiss-10) before the lordosis test. (*B*) Evaluation of lordosis behavior in experienced WT (n = 7) and Nos1$^{cre/+}$ (n = 6) female mice following Cre-dependent chemogenetic inhibition of nNOS^{VMH} neurons. Comparison analysis was performed within each group separately. Repeated-measures one-way ANOVA with Tukey's post hoc test. (*C* and *D*) Confocal images show Kiss1-green fluorescent protein (Kiss-GFP; in yellow) immunoreactivity and PR expression (in purple) in Kiss1^{RP3V} neurons in control and PAMH Kiss-GFP female mice (scale bars, 50 µm). Arrows show examples of PR expression in Kiss1-GFP–positive cells. Hollow white arrows point to GFP expression only. (*E* and *F*) Number of GFP immunoreactivity and coexpression between GFP and PR within Kiss1^{RP3V} neurons in control (n = 6) and PAMH (n = 5) female mice. Unpaired Student's t test. (*G*) Percentage of colocalization between GFP and PR within Kiss1^{RP3V} neurons in control (n = 6) and PAMH (n = 5) female mice. Mann–Whitney U test. Data are represented as mean ± SEM; *P < 0.05; **P < 0.01; ***P < 0.001; ****P < 0.0001.

behavioral experiments. We detected higher testosterone levels in PAMH female mice in estrus over the dark phase as compared to our previous reports (29) and others (55), in which diestrous mice were characterized only over the light phase. It remains unknown how precisely testosterone levels fluctuate over the estrous cycle and light:dark cycles in control and PCOS-like mice; however, these observations suggest that high testosterone levels during the estrous phase may disrupt progesterone-mediated actions in hypothalamic sex circuits of PCOS-like mice (56).

Our study reveals the presence of severe alterations in the display of mating behavior in PAMH mice, such as impaired lordosis and male-directed preference. Notably, impairment in lordosis behavior and enhanced sexual rejection were observed in both intact and ovariectomized PAMH mice supplemented with E2+P4, suggesting that intrinsic defects may arise from developmental disruptions in the PCOS-like condition, most likely impinging on central ovarian steroid hormone-sensitive neurons. Consistent with this hypothesis, we show that PCOS-like female mice have a robust loss of PR-expressing neurons in the VMH, which may profoundly affect the social interaction between mating partners and sexual performance. It is known that progesterone signaling via PR is required for the full display of lordosis behavior (37, 40). This requirement is placed in the hypothalamic module controlling sexual behavior in mammals, the VMH (15, 18, 19, 21, 41). PR^{VMH} neurons are a robust and required component of the female sexual brain for proper mating behavior (19). PR^{VMH} neurons are primed by estrogen, and structural circuit changes strengthen the connection between these neurons and their output within the RP3V region of the hypothalamus when female mice are receptive (15). This circuit plasticity is accompanied by an increase in the activity of PR^{VMH} neurons during both mating chemo-investigation and the display of lordosis (15). This development shows that PR^{VMH} neurons are a functionally relevant component of female sex circuits and that the loss of PR expression in the VMH may greatly contribute to sexual dysfunction in PCOS. Interestingly, among the three hypothalamic nuclei analyzed, the VMH contained the highest colocalization rate between PR and nNOS, with nearly 90% of PR cells coexpressing nNOS in control and PAMH mice, as opposed to 30 to 40% in the RP3V and only 5% in the ARN. These data further point to the VMH as a hot spot for NO signaling in progesterone-sensitive cells of the hypothalamus.

We provide evidence that there is a great loss of progesterone-sensitive nNOS^{VMH} neurons in PAMH female mice compared to controls. Progesterone actions in sex circuits are enhanced by drugs that increase cGMP levels, being a critical molecular output of NO actions in neuronal circuits (57). The NO-cGMP pathway is well characterized to mediate lordosis in rodents (22) but, to date, the functional relevance of nNOS^{VMH} neurons for this behavior has been unclear. We showed that treatment with sildenafil citrate, which impedes the degradation of cGMP, is not sufficient to promote the recovery of normal lordosis in PAMH mice, demonstrating the severity of NO deficiency in the VMH. A major finding from our study is that nNOS^{VMH} neurons are required to drive normal sexual behavior in female mice and that silencing these neurons using chemogenetics also enhances sexual rejection behaviors. Sexual rejection is profoundly modulated by sensorial inputs from the vomeronasal organ (VNO) pathways in female rodents (39, 49). For instance, the pheromone ESP22, which negatively affects lordosis, activates VNO-dependent

Downloaded from https://www.pnas.org by UNIVERSITEIT VAN AMSTERDAM UVA on April 14, 2025 from IP address 145.18.161.224.

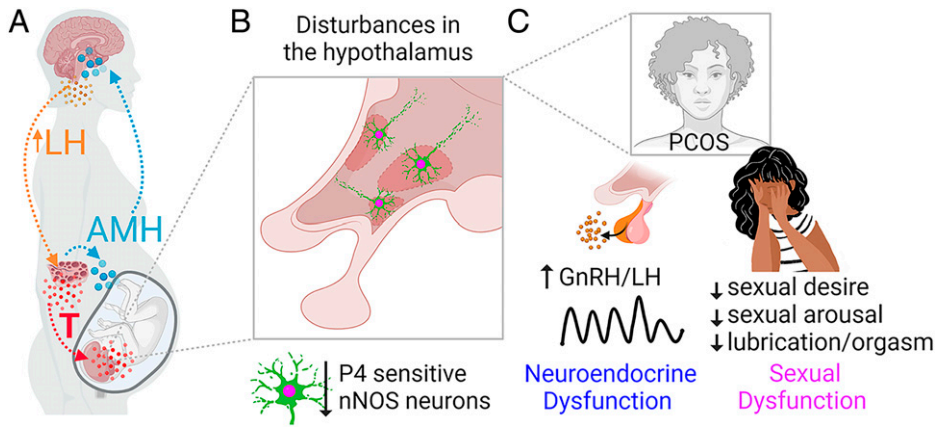

Fig. 5. Proposed AMH-mediated developmental drive of brain circuit abnormalities leading to the manifestation of sexual dysfunction in PCOS. (*A*) Excessive AMH production by PCOS ovaries accesses the mother's brain, leading to neuroendocrine dysfunction promoting high LH secretion. Exacerbated LH signaling favors enhanced ovarian testosterone (T) production, and high T levels act on the female fetal brain. AMH also deregulates placental steroidogenesis, which increases T bioavailability. (*B*) Prenatal AMH and testosterone excess reprogramming may mediate the loss of progesterone (P4)-sensitive nNOS neurons in different hypothalamic nuclei involved in reproductive and sexual competence. These brain circuit abnormalities may already be present during prepubertal life in girls with PCOS (28) and are carried over reproductive maturation. (*C*) Following the developmental reprogramming in hypothalamic circuitry, such as nNOS pathways, women with PCOS would be more likely to manifest both neuroendocrine and sexual dysfunction during adult reproductive life.

inhibitory GABAergic inputs to the vlVMH, enhancing sexual rejection in female mice (39). This evidence is in parallel with our findings illustrating the importance of proper vlVMH neuronal activity in female proceptive behavior. Loss of $nNOS^{VMH}$ neurons may impair the integration of sensorial inputs arriving in the VMH, leading to prolonged sexual rejection in PCOS-like mice, but whether these VNO pathways directly regulate $nNOS^{VMH}$ neuronal activity remains to be investigated. GABAergic transmission within the VMH has been reported to facilitate lordosis in female rodents (58), and projections from pdMeA GABA neurons to the vlVMH may mediate this facilitatory role (59). However, recent data showed that neuroendocrine dysfunction is highly associated with enhanced GABAergic inputs (29, 56) and signaling (26) in the hypothalamus in PCOS mouse models and with high levels of GABA in the cerebrospinal fluid of women with PCOS (60). Although it is tempting to speculate that excessive GABAergic transmission may override the facilitatory role of GABA in the VMH and be detrimental to lordosis behavior, future research should determine a definitive role of GABAergic pathways controlling female sexual behavior in the context of PCOS specifically.

Among their various afferents, $Kiss1^{RP3V}$ neurons have been recently proposed to contact the vlVMH to regulate female sexual behavior in mice (24). However, it is also known that PR^{VMH} neurons project back to the RP3V, displaying an estrous cycle–dependent functional connectivity between both nuclei (15). Here, using a pharmacological mechanistic approach, we showed that kisspeptin-mediated sexual effects are only relevant and dependent upon the proper function of $nNOS^{VMH}$ neurons. This finding strengthens the idea that $Kiss1^{RP3V}$ neurons are placed upstream of $nNOS^{VMH}$ neurons to drive lordosis behavior. However, we cannot exclude the possibility that $nNOS^{VMH}$ neurons also impinge upon $Kiss1^{RP3V}$ neuronal activity, forming a homeostatic loop between the RP3V and the VMH over the control of female sexual behavior in mice. Further dissection showed that PAMH female mice present a robust reduction of progesterone-sensitive $Kiss1^{RP3V}$ neurons, which most likely contributes to the loss of kisspeptin–$nNOS^{VMH}$ coupling required for proper sexual function in PCOS.

Recent studies have suggested that the PAMH-induced reproductive phenotype is mediated by androgen signaling at the level of kisspeptin cells (54), and a functional androgen receptor (AR) in neurons is required for the presentation of PCOS-like features in female mice (61). Previous works have also shown that exposure to high androgen levels lowers the hypothalamic expression of nNOS (62) and that AR signaling and its interactions with estrogen receptor alpha have profound organizational effects on the number of nNOS neurons in limbic areas in mice (46, 63). Consistently, we found that PAMH female mice presented a loss of nNOS expression in the hypothalamic R3PV, VMH, and ARN. However, we did not detect any significant changes in the number of nNOS-expressing neurons distributed in other the hypothalamic and limbic regions of PAMH brains as compared to those in the control animals, suggesting that such loss is region-specific and that the lack of NO in these areas could disrupt normal neurotransmitter function and impact sexual behavior.

We hypothesize that in PCOS-like animals, perinatal exposure to androgen excess has organizational actions on nNOS-ir cell numbers in hypothalamic areas associated with the control of reproductive functions and sexual behavior, thus triggering developmental brain circuit abnormalities with detrimental outcomes over the adult reproductive life and finally affecting proper female sexual performance and neuroendocrine functions (Fig. 5). Indeed, our neuroanatomical data were also associated with the detection of high LH pulses in estrous PAMH mice, implying that the loss of homeostatic control of the GnRH/LH secretion in PAMH may be linked to impaired progesterone signaling at the central level as previously documented in women with PCOS (64) and other PCOS animal models (56). The present investigation also revisited the expression of $Kiss1^{RP3V}$ neurons in PAMH female mice and documented that these mice have a profound loss of progesterone-sensitive $Kiss1^{RP3V}$ neurons. This particular group of $Kiss1^{RP3V}$ neurons is pivotal to the preovulatory GnRH/LH surge (65, 66), and disruptions in this population are likely to contribute to fertility problems in a PCOS-like condition.

The disruption of NO signaling in the RP3V and ARN of PAMH female mice may be related to the control of GnRH neuron function as previously discovered by our group (67, 68) and others (69), showing that NO inhibits the firing pattern of GnRH neurons and modulates the pulsatile secretion of GnRH (67). Notably, PAMH animals present chronically increased spontaneous GnRH neuronal activity together with exacerbated

Downloaded from https://www.pnas.org by UNIVERSITEIT VAN AMSTERDAM UVA on April 14, 2025 from IP address 145.18.161.224.

LH pulse secretion (29), and we now provide evidence of a strong reduction in the number of nNOS-expressing neurons in these animals, which could account for the accelerated GnRH/LH pulse frequency. Future works are thus required to assess whether NO supplementation may restore the neuroendocrine and reproductive alterations of PCOS-like animals. Interestingly, clinical meta-analysis data showed that PCOS is strongly associated with low serum or plasma levels of NO metabolites (42, 43). However, it remains unknown whether an attenuated NO pathway is present in PCOS brain circuits. Moreover, pharmacological strategies that increase NO levels have been shown to hold promising therapeutic potential for the reproductive alterations of PCOS as they improved menstrual cyclicity, ovulation (70, 71), and pregnancy rates (71) in women with PCOS.

Here, we provide evidence that the use of NO donors (i.e., SNAP) ameliorates sexual dysfunction in a preclinical PCOS model. Changes in cFOS expression within the hypothalamic and limbic systems driven by SNAP administration suggest that NO supplementation may recover sexual function by reinstating normal circuitry response to a sexual encounter in our model. It will be interesting in the future to determine whether women with PCOS or women affected by hypoactive sexual desire disorder, the most severe form of low sexual drive (72), present altered central levels of NO and/or nNOS circuitry, and whether they could eventually benefit from NO-based therapeutic options.

In conclusion, our results have broad repercussions for our understanding of developmental reprogramming in the female brain leading to disturbances in hypothalamic circuitry, driving sexual dysfunction in PCOS, and provide grounds for prospective therapeutical venues aimed at correcting these defects.

Materials and Methods

Animals. Mice were housed under specific pathogen-free conditions in a temperature-controlled room (21°C–22 °C) and ad libitum access to food and drinking water. Unless stated in the text, mice were kept under an inverted 12-h light:dark cycle with lights off from 9:00 am to 9:00 pm. All experiments were performed using adult (ages 2–5 mo) wild-type mice, and transgenic lines are described in *SI Appendix*. Animal care and experimental design were carried out under the guidelines established by the European Council Directive of September 22, 2010 (2010/63/EU) and under ethical protocol number APAFIS#29172–2020121811279767 v5 from the Institutional Ethics Committees of Care and Use of Experimental Animals of the University of Lille, France.

PAMH Treatment. The generation of PAMH female mice was carried out according to a previous report (29) and is detailed in *SI Appendix*.

Assessment of Reproductive Status, LH Pulse Profiling, and Blood Sampling. Estrous cycle pattern was assessed in adult control and PAMH mice as stated elsewhere (73) and is detailed in the *SI Appendix*.

Hormone Measurements and Analysis. Blood sampling for both LH and testosterone measurements was collected over the dark phase 3 h after the lights were turned off. Blood LH levels were determined using a well-established enzyme-linked immunosorbent assay (ELISA) method (74) (*SI Appendix*). Plasma testosterone levels were measured in duplicates using a commercial ELISA kit (Demeditec Diagnostics, GmbH, DEV9911) according to the manufacturer's instructions. The assay sensitivity of this mouse testosterone ELISA was 0.066 ng/mL, and the intra-assay coefficient of variation was 10.4%.

Immunohistochemistry, Image Acquisition, and Analysis. Tissue preparation for immunohistochemistry is detailed in *SI Appendix*. Immunohistochemistry was performed as described elsewhere (28, 75). Primary antibodies were used at the following respective concentrations: polyclonal sheep anti-nNOS (1:2,000; generous gift from Dr. Piers C. Emson and validated elsewhere [76]), polyclonal rabbit anti-PR (1:500; Sigma; SAB4502184), rabbit anti-red fluorescent protein (1:500; Rockland Immunochemicals, Inc.; 600-401-379), polyclonal chicken anti-GFP (1:1,000; Aves Labs Inc., GFP-1020), and polyclonal rabbit anti-cFOS (Synaptic Systems GmbH; 226 008). Brain sections were incubated with a mixture of primary antibodies and 2% normal donkey serum in incubation solution (0.25% bovine serum albumin with 0.3% Triton in TBS) over 48 h at 4 °C. Following washes with TBS, brain sections were incubated with secondary antibodies. Alexa Fluor 488 donkey anti-sheep (A11015), Alexa Fluor 647 donkey anti-rabbit, (A31573), and Alexa Fluor 568 donkey anti-rabbit (A10042) were all purchased from Thermo Fisher Scientific Inc. and used at 1:400 dilution in TBS solution. Alexa Fluor 488 donkey anti-chicken (Jackson ImmunoResearch Labs; 703-545-155) was used at 1:500 dilution in TBS solution. Sections were mounted onto glass slides and left to dry until covered with Fluoromount-G with DAPI (Invitrogen/Thermo Fisher Scientific Inc.; 00-4959-52), and coverslipped. Two representative brain sections from each brain region were chosen from each animal for image acquisition and immunohistological analysis. Detailed procedures for image acquisition and cFOS quantification are provided in *SI Appendix*.

Ovariectomy and Ovarian Steroid Hormone Supplementation. Adult female mice (age 3 mo) were ovariectomized under 4% isoflurane anesthesia with constant airflow. Two weeks following surgery and recovery, female mice were primed with E2+P4 to have high sexual receptivity based on previous reports (77). To this end, mice received subcutaneous (s.c.) injections of 0.5 μg/50 μL estradiol benzoate (Sigma-Aldrich; E8515) 48 h and 24 h prior to the lordosis test, and a single s.c. injection of 500 μg/50 μL progesterone (Sigma-Aldrich; P0130) 3 to 4 h before the lordosis test. Both drugs were diluted in sesame oil at least one day before the protocol commenced.

Female Sexual Behavior Test. Estrous female mice were tested for lordosis behavior over the dark phase following previously reported protocols (24, 37) and as described in *SI Appendix*. During the annotation of sexual behavior, we also assessed sexual rejection behaviors over the same period (*SI Appendix*). All behavior tests were videotaped and manually annotated using Behavioral Observation Research Interactive Software (78).

Mate Preference Test. The mate preference test assessed the response of female mice to sensory stimuli to same- and opposite-sex counterparts. Technical details are described in *SI Appendix*.

EPM Test. The EPM test was employed as previously reported elsewhere (36), and details are provided in *SI Appendix*.

Chemogenetic Manipulations (Viral Transfection, Stereotaxic Injections, and Behavioral Assessment). The AAV9 hM4D DREADD (AAV-hSyn-DIO-hM4D(Gi)-mCherry) (titer = 4.5×10^{12} vg/mL; Addgene; 44362-AAV9) was stereotaxically injected into the vlVMH (*SI Appendix*) of *Nos1-ires-cre* female mice under 4% isoflurane anesthesia with constant airflow. The lordosis test was carried out as described above with sexually experienced female mice after three lordosis test trials. Female mice received an intraperitoneal (i.p.) injection with 100 μL CNO (Tocris; 6329) at a dose of 3 mg/kg diluted in sterile saline one hour before behavioral assessment. Each mouse received either CNO or saline (vehicle) in a random order, and the two behavioral assessments were performed 10 days apart.

Pharmacological Treatments. SNAP: Female mice received an s.c. injection with 8 mg/kg SNAP (Sigma-Aldrich; N3398) diluted in 100 μL saline 15 min before behavioral testing, and the chosen dose was based on previous reports (24). Kisspeptin: Female mice received an s.c. injection with 0.52 μg/kg kisspeptin-10 (Kiss-10; rodent metastin [45–54] amide; GeneCust YY-10-NH2) diluted in 100 μL saline 30 min before the behavioral test based on previous reports (24). Sildenafil citrate: Female mice received an i.p. injection with 15 mg/kg sildenafil citrate (Sigma-Aldrich; 171599–83-0) 1 h before behavioral assessment based on previous trials from our laboratory. Sildenafil citrate was first diluted in DMSO to make up a stock solution of 25 mg/mL and further diluted with sterile saline to make up a working solution of 15 mg/mL for s.c. injection on the day of the injection.

Data Analysis and Statistics. Statistical analysis was performed with PRISM software 8.0 (GraphPad Software, San Diego, CA). Normal distribution was determined with the Shapiro–Wilk normality test for all samples before any group analysis. Sample sizes were chosen according to standard practices and are shown in each figure legend. Investigators were not blinded to the group

Downloaded from https://www.pnas.org by UNIVERSITEIT VAN AMSTERDAM UVA on April 14, 2025 from IP address 145.18.161.224.

allocation or drug treatment; however, each mouse was randomly chosen to receive different treatments on different days. We used the Mann–Whitney *U* test to compare two experimental groups in which unpaired samples were not normally distributed. For normally distributed unpaired samples, we used a two-tailed Student's *t* test. Paired samples were analyzed using the Wilcoxon signed-rank test or a repeated-measures one-way ANOVA. Group analysis with two nominal predictor variables used two-way ANOVA with either Tukey's or Sidak's posthoc test. Statistical significance was accepted when $P < 0.05$.

Data Availability. All study data are included in the article and/or *SI Appendix*.

ACKNOWLEDGMENTS. We thank A. Loyens and Dr. G. Ternier for their great assistance, C. Laloux, and the Lille In Vivo Imaging and Functional Exploration platform (University of Lille, CNRS, INSERM, CHU Lille, Institut Pasteur of Lille, US41-UMS2014 PLBS, France) for technical support during behavioral assessment experiments. This work was supported by the European Research Council (ERC) under the European Union's Horizon 2020 research and innovation program (ERC-2016-CoG to P.G., Grant Agreement No. 725149/REPRODAMH), by the European Union's Horizon 2020 Research and Innovation Programme under grant Agreement No. 847941/miniNO to K.C. and V.P., and by the INSERM-France (Grant Number U1172) to P.G. and V.P. We thank BioRender.com for the design tools used to create the scientific illustrations. We thank Professor Bryan Roth and his research group for providing the pAAV-hSyn-DIO-hM4D(Gi)-mCherry (Addgene plasmid 44362).

Author affiliations: [a]Laboratory of Development and Plasticity of the Neuroendocrine Brain, Lille Neuroscience & Cognition UMR-S1172, FHU 1000 days for health, Université de Lille, CHU Lille, INSERM, Lille, 59000, France; and [b]Department of Pharmacology and Toxicology, Center for Molecular Signaling, Saarland University School of Medicine, Homburg, 66421, Germany

Author contributions: M.S.B.S., V.P., and P.G. designed research; M.S.B.S., L.D., S.T., N.E.H.M., V.D., K.C., and Q.Y. performed research; U.B. and V.P. contributed new reagents/analytic tools; M.S.B.S., S.T., N.E.H.M., Q.Y., and P.G. analyzed data; and M.S.B.S. and P.G. wrote the paper.

1. D. Lizneva *et al.*, Criteria, prevalence, and phenotypes of polycystic ovary syndrome. *Fertil. Steril.* **106**, 6–15 (2016).
2. R. Azziz *et al.*, Polycystic ovary syndrome. *Nat. Rev. Dis. Primers* **2**, 16057 (2016).
3. Rotterdam ESHRE/ASRM-Sponsored PCOS Consensus Workshop Group, Revised 2003 consensus on diagnostic criteria and long-term health risks related to polycystic ovary syndrome. *Fertil. Steril.* **81**, 19–25 (2004).
4. D. A. Dumesic *et al.*, Scientific statement on the diagnostic criteria, epidemiology, pathophysiology, and molecular genetics of polycystic ovary syndrome. *Endocr. Rev.* **36**, 487–525 (2015).
5. A. H. Rellini *et al.*, Differences in sexual desire between women with clinical versus biochemical signs of hyperandrogenism in polycystic ovarian syndrome. *Horm. Behav.* **63**, 65–71 (2013).
6. M. Steinberg Weiss *et al.*, Lifestyle modifications alone or combined with hormonal contraceptives improve sexual dysfunction in women with polycystic ovary syndrome. *Fertil. Steril.* **115**, 474–482 (2021).
7. D. W. Stovall, J. L. Scriver, A. H. Clayton, C. D. Williams, L. M. Pastore, Sexual function in women with polycystic ovary syndrome. *J. Sex. Med.* **9**, 224–230 (2012).
8. H. Pastoor *et al.*, Sexual function in women with polycystic ovary syndrome: A systematic review and meta-analysis *Reprod. Biomed Online.* **37**, 750–760 (2018).
9. X. Tian *et al.*, Sexual function in Chinese women with polycystic ovary syndrome and correlation with clinical and biochemical characteristics. *Reprod. Sci.* **28**, 3181–3192 (2021).
10. J. G. Pfaus, S. L. Jones, L. M. Flanagan-Cato, J. D. Blaustein, "Female sexual behavior" in *Knobil and Neill's Physiology of Reproduction*, T. M. Plant, A. J. Zeleznik, Eds. (Academic Press, 2015), ed. 4, pp. 2287–2370.
11. K. M. Lenz, M. M. McCarthy, Organized for sex–Steroid hormones and the developing hypothalamus. *Eur. J. Neurosci.* **32**, 2096–2104 (2010).
12. R. B. Simerly, Wired for reproduction: Organization and development of sexually dimorphic circuits in the mammalian forebrain. *Annu. Rev. Neurosci.* **25**, 507–536 (2002).
13. C. A. Cornil, G. F. Ball, J. Balthazart, T. D. Charlier, Organizing effects of sex steroids on brain aromatase activity in quail. *PLoS One* **6**, e19196 (2011).
14. K. Chachlaki, J. Garthwaite, V. Prevot, The gentle art of saying NO: How nitric oxide gets things done in the hypothalamus. *Nat. Rev. Endocrinol.* **13**, 521–535 (2017).
15. S. Inoue *et al.*, Periodic remodeling in a neural circuit governs timing of female sexual behavior. *Cell* **179**, 1393–1408.e16 (2019).
16. B. Zempo, T. Karigo, S. Kanda, Y. Akazome, Y. Oka, Morphological analysis of the axonal projections of EGFP-labeled ESR1-expressing neurons in transgenic female medaka. *Endocrinology* **159**, 1228–1241 (2018).
17. K. Sinchak *et al.*, Modulation of the arcuate nucleus-medial preoptic nucleus lordosis regulating circuit: A role for GABAB receptors. *Horm. Behav.* **64**, 136–143 (2013).
18. K. Nomoto, S. Q. Lima, Enhanced male-evoked responses in the ventromedial hypothalamus of sexually receptive female mice. *Curr. Biol.* **25**, 589–594 (2015).
19. C. F. Yang *et al.*, Sexually dimorphic neurons in the ventromedial hypothalamus govern mating in both sexes and aggression in males. *Cell* **153**, 896–909 (2013).
20. D. W. Kim *et al.*, Multimodal analysis of cell types in a hypothalamic node controlling social behavior. *Cell* **179**, 713–728.e17 (2019).
21. D. W. Pfaff, Y. Sakuma, Facilitation of the lordosis reflex of female rats from the ventromedial nucleus of the hypothalamus. *J. Physiol.* **288**, 189–202 (1979).
22. S. K. Mani *et al.*, Nitric oxide mediates sexual behavior in female rats. *Proc. Natl. Acad. Sci. U.S.A.* **91**, 6468–6472 (1994).
23. Y. Bentefour, J. Bakker, Kisspeptin signaling and nNOS neurons in the VMHvl modulate lordosis behavior but not mate preference in female mice. *Neuropharmacology* **198**, 108762 (2021).
24. V. Hellier *et al.*, Female sexual behavior in mice is controlled by kisspeptin neurons. *Nat. Commun.* **9**, 400 (2018).
25. O. González-Flores, A. M. Etgen, The nitric oxide pathway participates in estrous behavior induced by progesterone and some of its ring A-reduced metabolites. *Horm. Behav.* **45**, 50–57 (2004).
26. S. D. Sullivan, S. M. Moenter, Prenatal androgens alter GABAergic drive to gonadotropin-releasing hormone neurons: Implications for a common fertility disorder. *Proc. Natl. Acad. Sci. U.S.A.* **101**, 7129–7134 (2004).
27. H. Hedström *et al.*, Women with polycystic ovary syndrome have elevated serum concentrations of and altered GABA(A) receptor sensitivity to allopregnanolone. *Clin. Endocrinol. (Oxf.)* **83**, 643–650 (2015).
28. M. S. B. Silva, M. Prescott, R. E. Campbell, Ontogeny and reversal of brain circuit abnormalities in a preclinical model of PCOS. *JCI Insight* **3**, 99405 (2018).
29. B. Tata *et al.*, Elevated prenatal anti-Müllerian hormone reprograms the fetus and induces polycystic ovary syndrome in adulthood. *Nat. Med.* **24**, 834–846 (2018).
30. N. E. H. Mimouni *et al.*, Polycystic ovary syndrome is transmitted via a transgenerational epigenetic process. *Cell Metab.* **33**, 513–530.e8 (2021).
31. T. T. Piltonen *et al.*, Circulating antiMüllerian hormone and steroid hormone levels remain high in pregnant women with polycystic ovary syndrome at term. *Fertil. Steril.* **111**, 588–596.e1 (2019).
32. E. Stener-Victorin *et al.*, Animal models to understand the etiology and pathophysiology of polycystic ovary syndrome. *Endocr. Rev.* **41**, bnaa010 (2020).
33. T. L. Daniels, S. L. Berga, Resistance of gonadotropin releasing hormone drive to sex steroid-induced suppression in hyperandrogenic anovulation. *J. Clin. Endocrinol. Metab.* **82**, 4179–4183 (1997).
34. R. Azziz *et al.*; Task Force on the Phenotype of the Polycystic Ovary Syndrome of The Androgen Excess and PCOS Society, The Androgen Excess and PCOS Society criteria for the polycystic ovary syndrome: The complete task force report. *Fertil. Steril.* **91**, 456–488 (2009).
35. L. G. Cooney, I. Lee, M. D. Sammel, A. Dokras, High prevalence of moderate and severe depressive and anxiety symptoms in polycystic ovary syndrome: A systematic review and meta-analysis. *Hum. Reprod.* **32**, 1075–1091 (2017).
36. A. A. Walf, C. A. Frye, The use of the elevated plus maze as an assay of anxiety-related behavior in rodents. *Nat. Protoc.* **2**, 322–328 (2007).
37. S. K. Mani *et al.*, Dopamine requires the unoccupied progesterone receptor to induce sexual behavior in mice. *Mol. Endocrinol.* **10**, 1728–1737 (1996).
38. C. Lenschow, S. Q. Lima, In the mood for sex: Neural circuits for reproduction. *Curr. Opin. Neurobiol.* **60**, 155–168 (2020).
39. T. Osakada *et al.*, Sexual rejection via a vomeronasal receptor-triggered limbic circuit. *Nat. Commun.* **9**, 4463 (2018).
40. J. P. Lydon *et al.*, Mice lacking progesterone receptor exhibit pleiotropic reproductive abnormalities. *Genes Dev.* **9**, 2266–2278 (1995).
41. G. J. Romano, A. Krust, D. W. Pfaff, Expression and estrogen regulation of progesterone receptor mRNA in neurons of the mediobasal hypothalamus: An in situ hybridization study. *Mol. Endocrinol.* **3**, 1295–1300 (1989).
42. C. Meng, Nitric oxide (NO) levels in patients with polycystic ovary syndrome (PCOS): A meta-analysis. *J. Int. Med. Res.* **47**, 4083–4094 (2019).
43. M. B. Krishna *et al.*, Impaired arginine metabolism coupled to a defective redox conduit contributes to low plasma nitric oxide in polycystic ovary syndrome. *Cell. Physiol. Biochem.* **43**, 1880–1892 (2017).
44. C. L. Pastor, M. L. Griffin-Korf, J. A. Aloi, W. S. Evans, J. C. Marshall, Polycystic ovary syndrome: Evidence for reduced sensitivity of the gonadotropin-releasing hormone pulse generator to inhibition by estradiol and progesterone. *J. Clin. Endocrinol. Metab.* **83**, 582–590 (1998).
45. P. B. Chen *et al.*, Sexually dimorphic control of parenting behavior by the medial amygdala. *Cell* **176**, 1206–1221.e18 (2019).
46. E. M. Scordalakes, S. J. Shetty, E. F. Rissman, Roles of estrogen receptor α and androgen receptor in the regulation of neuronal nitric oxide synthase. *J. Comp. Neurol.* **453**, 336–344 (2002).
47. N. S. Canteras, R. B. Simerly, L. W. Swanson, Organization of projections from the ventromedial nucleus of the hypothalamus: A phaseolus vulgaris-leucoagglutinin study in the rat. *J. Comp. Neurol.* **348**, 41–79 (1994).
48. L. Lo *et al.*, Connectional architecture of a mouse hypothalamic circuit node controlling social behavior. *Proc. Natl. Acad. Sci. U.S.A.* **116**, 7503–7512 (2019).
49. K. K. Ishii *et al.*, A labeled-line neural circuit for pheromone-mediated sexual behaviors in mice. *Neuron* **95**, 123–137.e8 (2017).
50. S. da Silva Pacheco, T. Araujo Rondini, J. Cioni Bittencourt, C. Fuzeti Elias, Neurons expressing estrogen receptor α differentially innervate the periaqueductal gray matter of female rats. *J. Chem. Neuroanat.* **97**, 33–42 (2019).
51. L. H. Calizo, L. M. Flanagan-Cato, Hormonal-neural integration in the female rat ventromedial hypothalamus: Triple labeling for estrogen receptor-α, retrograde tract tracing from the periaqueductal gray, and mating-induced Fos expression. *Endocrinology* **144**, 5430–5440 (2003).
52. O. Iyilikci, J. Balthazart, G. F. Ball, Medial preoptic regulation of the ventral tegmental area related to the control of sociosexual behaviors. *eNeuro* **3**, ENEURO.0283-16.2016 (2017).
53. N. Bellefontaine *et al.*, Leptin-dependent neuronal NO signaling in the preoptic hypothalamus facilitates reproduction. *J. Clin. Invest.* **124**, 2550–2559 (2014).
54. E. V. Ho *et al.*, Reproductive deficits induced by prenatal antiMüllerian hormone exposure require androgen receptor in kisspeptin cells. *Endocrinol.* **162**, bqab197 (2021).
55. A. M. Moore, M. Prescott, R. E. Campbell, Estradiol negative and positive feedback in a prenatal androgen-induced mouse model of polycystic ovarian syndrome. *Endocrinology* **154**, 796–806 (2013).

Downloaded from https://www.pnas.org by UNIVERSITEIT VAN AMSTERDAM UVA on April 14, 2025 from IP address 145.18.161.224.

56. A. M. Moore, M. Prescott, C. J. Marshall, S. H. Yip, R. E. Campbell, Enhancement of a robust arcuate GABAergic input to gonadotropin-releasing hormone neurons in a model of polycystic ovarian syndrome. *Proc. Natl. Acad. Sci. U.S.A.* **112**, 596–601 (2015).
57. H. P. Chu, J. C. Morales, A. M. Etgen, Cyclic GMP may potentiate lordosis behaviour by progesterone receptor activation. *J. Neuroendocrinol.* **11**, 107–113 (1999).
58. M. M. McCarthy, K. F. Malik, H. H. Feder, Increased GABAergic transmission in medial hypothalamus facilitates lordosis but has the opposite effect in preoptic area. *Brain Res.* **507**, 40–44 (1990).
59. C. S. Johnson, W. Hong, P. E. Micevych, Posterodorsal medial amygdala regulation of female social behavior: GABA versus glutamate projections. *J. Neurosci.* **41**, 8790–8800 (2021).
60. J. F. Kawwass, K. M. Sanders, T. L. Loucks, L. C. Rohan, S. L. Berga, Increased cerebrospinal fluid levels of GABA, testosterone and estradiol in women with polycystic ovary syndrome. *Hum. Reprod.* **32**, 1450–1456 (2017).
61. A. S. L. Caldwell *et al.*, Neuroendocrine androgen action is a key extraovarian mediator in the development of polycystic ovary syndrome. *Proc. Natl. Acad. Sci. U.S.A.* **114**, E3334–E3343 (2017).
62. R. Singh, S. Pervin, J. Shryne, R. Gorski, G. Chaudhuri, Castration increases and androgens decrease nitric oxide synthase activity in the brain: Physiologic implications. *Proc. Natl. Acad. Sci. U.S.A.* **97**, 3672–3677 (2000).
63. M. Edelmann, C. Wolfe, E. M. Scordalakes, E. F. Rissman, S. Tobet, Neuronal nitric oxide synthase and calbindin delineate sex differences in the developing hypothalamus and preoptic area. *Dev. Neurobiol.* **67**, 1371–1381 (2007).
64. C. A. Eagleson *et al.*, Polycystic ovarian syndrome: Evidence that flutamide restores sensitivity of the gonadotropin-releasing hormone pulse generator to inhibition by estradiol and progesterone. *J. Clin. Endocrinol. Metab.* **85**, 4047–4052 (2000).
65. S. B. Z. Stephens *et al.*, Absent progesterone signaling in kisspeptin neurons disrupts the LH surge and impairs fertility in female mice. *Endocrinology* **156**, 3091–3097 (2015).
66. M. A. Mohr, L. A. Esparza, P. Steffen, P. E. Micevych, A. S. Kauffman, Progesterone receptors in AVPV kisspeptin neurons are sufficient for positive feedback induction of the LH surge. *Endocrinology* **162**, bqab161.
67. J. Clasadonte, P. Poulain, J.-C. Beauvillain, V. Prevot, Activation of neuronal nitric oxide release inhibits spontaneous firing in adult gonadotropin-releasing hormone neurons: A possible local synchronizing signal. *Endocrinology* **149**, 587–596 (2008).
68. N. K. Hanchate *et al.*, Kisspeptin-GPR54 signaling in mouse NO-synthesizing neurons participates in the hypothalamic control of ovulation. *J. Neurosci.* **32**, 932–945 (2012).
69. S. Constantin, D. Reynolds, A. Oh, K. Pizano, S. Wray, Nitric oxide resets kisspeptin-excited GnRH neurons via PIP2 replenishment. *Proc. Natl. Acad. Sci. U.S.A.* **118**, e2012339118 (2021).
70. A. Masha *et al.*, Prolonged treatment with N-acetylcysteine and L-arginine restores gonadal function in patients with polycystic ovary syndrome. *J. Endocrinol. Invest.* **32**, 870–872 (2009).
71. A. Mahran, A. Abdelmeged, H. Shawki, A. Moheyelden, A. M. Ahmed, Nitric oxide donors improve the ovulation and pregnancy rates in anovulatory women with polycystic ovary syndrome treated with clomiphene citrate: A RCT. *Int. J. Reprod. Biomed. (Yazd)* **14**, 9–14 (2016).
72. R. E. Nappi *et al.*, Management of hypoactive sexual desire disorder in women: Current and emerging therapies. *Int. J. Womens Health* **2**, 167–175 (2010).
73. C. S. Caligioni, Assessing reproductive status/stages in mice. *Curr. Protoc. Neurosci.* **Appendix 4**, Appendix-4I (2009).
74. F. J. Steyn *et al.*, Development of a methodology for and assessment of pulsatile luteinizing hormone secretion in juvenile and adult male mice. *Endocrinology* **154**, 4939–4945 (2013).
75. K. Chachlaki *et al.*, Phenotyping of nNOS neurons in the postnatal and adult female mouse hypothalamus. *J. Comp. Neurol.* **525**, 3177–3189 (2017).
76. A. E. Herbison, S. X. Simonian, P. J. Norris, P. C. Emson, Relationship of neuronal nitric oxide synthase immunoreactivity to GnRH neurons in the ovariectomized and intact female rat. *J. Neuroendocrinol.* **8**, 73–82 (1996).
77. J. A. Johansen, L. G. Clemens, A. A. Nunez, Characterization of copulatory behavior in female mice: Evidence for paced mating. *Physiol. Behav.* **95**, 425–429 (2008).
78. O. Friard, M. Gamba, BORIS: A free, versatile open-source event-logging software for video/audio coding and live observations. *Methods Ecol. Evol.* **7**, 1325–1330 (2016).

Downloaded from https://www.pnas.org by UNIVERSITEIT VAN AMSTERDAM UVA on April 14, 2025 from IP address 145.18.161.224.